Restoration of Lung Sound Signals Using a Hybrid Wavelet-based Approach

Chang Sheng Lee, *Student Member*, *IEEE*, Minghui Li, *Senior Member, IEEE*, Yaolong Lou, *Senior Member, IEEE,* and Ravinder Dahiya, *Fellow, IEEE*

***Abstract*—A unique and ideal integration of wavelet-based total variation (WATV) and empirical Wiener denoising method is proposed in this paper to significantly enhance the signal-to-noise ratio (SNR) while preserving the characteristics of a lung sound signal. While individual wavelet-based denoising filters based on a single basis function have been employed in the past, the outcome has been unsatisfactory because only significant (signal) wavelet coefficients are considered for denoising analysis. The new WATV-Wiener hybrid technique, proposed here, takes into account both significant and insignificant (noise) wavelet coefficients of the noisy signal. An intensive analysis of selecting and fine-tuning the WATV-Wiener filter parameters is presented here through the simulation studies. The WATV-Wiener filter applied here onto different one-dimensional lung sound signals of different noise levels has led to an optimal root mean square error compared to seven other state-of-the-art filters reported in the literature. The optimal parameters achieved through our simulation studies led to a 3–20 dB improvement in SNR, and the average SNR was improved by 4–30 dB in our experiment. We also observed that the WATV-Wiener filter is less sensitive to the variation of SNR values of the input signal. Furthermore, the WATV-Wiener filter obtains similar SNR performance between continuous piecewise signal (wheeze) and noncontinuous piecewise signal (crackle) in both simulation and experimental studies.**

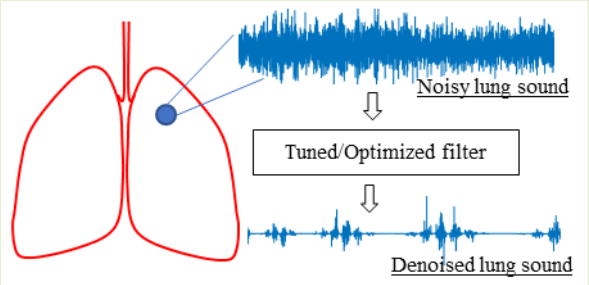

***Index Terms*—Denoising, lung sound signal, signal to noise ratio, signal estimation, Wavelets, Wiener filter.**

I. Introduction

The respiratory sounds carry the signature of the health status of the lungs and can be used for diagnosing respiratory diseases. For example, auscultation serves as a reference point and is frequently used by doctors and clinicians to 'listen' to weird lung sounds and patterns. Whilst auscultation is widely adopted, it is not easy to use as issues such as variability and dependent on inter-listeners medical and diagnostic skills. In this regard, the computer-based lung sound techniques are attractive as they eliminate the subjective nature and provide a more reliable approach to assessing lung function [1]–[3]. However, in lung sound recording, noise source such as ambient noise is an inevitable interference that can obscure the existence of interesting sound trends. Interference obstructs the computer-based lung sound algorithm's applicability or results in undesirable false positives; thus, noise reduction or denoising is crucial in lung sound signal processing.

To address these issues, we present here an indirect and optimal integration of wavelet-based total variation filter and wavelet-based empirical Wiener filter (WATV-Wiener) to smoothen the denoised signal (Fig. 1) and significantly improve the signal-to-noise ratio (SNR) and root mean square error (RMSE) of the denoised signal, which are crucial for an accurate assessment. SNR, in our case, reflects the denoised signal strength in relation to noise without compromising the frequency components of interest contained in the lung sound signal. Literature has confirmed that clinicians were able to distinctly identify airway diseases such as asthma, chronic obstructive pulmonary disease (COPD), and fluid around the lungs (pneumonia) from captured interesting signal waveform characteristics such as wheeze and crackle [3]–[5] compared to pre-denoised data, typically on conditions that the SNR is enhanced in the order of 4–20 dB [2], [6]–[8]. RMSE results

This Manuscript submitted XXX XX, 2022. This work was supported and funded by the Singapore Economic Development Board (EDB).

An earlier version of this paper was presented at the IEEE 40th International Conference on Consumer Electronics Conference. https://ieeexplore.ieee.org/document/9730394

Chang Sheng Lee is with the James Watt School of Engineering, University of Glasgow, Glasgow G12 8QQ, United Kingdom, and with Global Technology Integration department, Hill-Rom Services Pte Ltd, 1 Yishun Ave 7 Singapore 768923 (e-mail: changsheng.lee@hillrom.com).

Minghui Li is with the James Watt School of Engineering, University of Glasgow, Glasgow G12 8QQ, United Kingdom (e-mail: David.Li@glasgow.ac.uk).

Yaolong Lou is with the Global Technology Integration department, Hill-Rom Services Pte Ltd, 1 Yishun Ave 7 Singapore 768923 (e-mail: Yaolong.Lou@hillrom.com).

Ravinder Dahiya is with Bendable Electronics and Sensing Technologies (BEST) Group, James Watt School of Engineering, University of Glasgow, Glasgow G12 8QQ, United Kingdom (e-mail: Ravinder.Dahiya@glasgow.ac.uk).

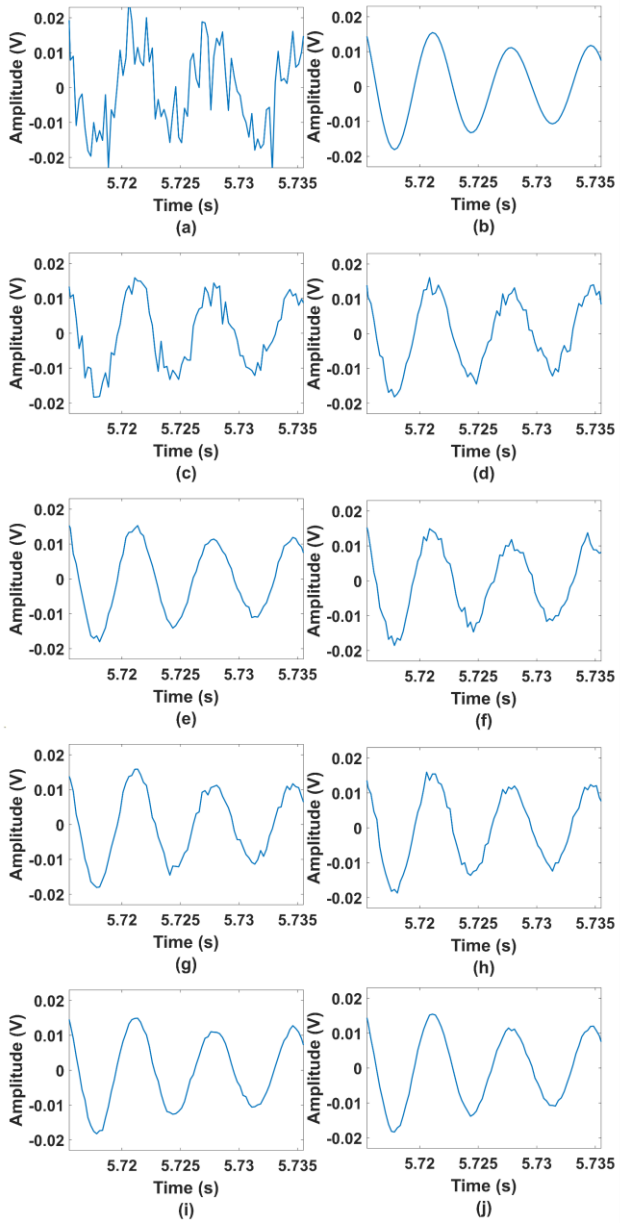

Fig. 1. Comparing (a) the noisy signal, (b) the noise-free signal, and the output of normalized denoised lung sound signal typically for lung health assessment and diagnostic through (c) Bandpass filter; (d) Hard thresholding filter; (e) Serial filter; (f) Soft thresholding filter; (g) Savitzky-Golay filter; (h) Total variation filter; (i) Wavelet-based total variation filter; and (j) Proposed filter – WATV-Wiener filter.

reflect the filter capability in denoising and retaining significant characteristics of lung sound. Inefficient parameter selection resulting in overly suppressed denoised signal may result in high SNR, despite the filter introducing obvious distortions resulting in undesirable RMSE results. As a result, RMSE is also a crucial criterion for determining if the denoising filter keeps the desired waveform characteristics of interest.

In addition, a comprehensive investigation was conducted on ideal parameters selection to facilitate the optimization of our proposed WATV-Wiener technique, particularly in the lung sound signal domain, as only parameters estimates were available in the literature, and no case studies on how the parameters adjustment affected the filter performance were performed or discussed [9], [10].

To thoroughly evaluate the WATV-Wiener filter, we compared the proposed filter with a range of state-of-the-art lung sound signal denoising techniques, which had achieved either optimal SNR or RMSE performance, or achieved good results in both SNR and RMSE in the literature [6], [9]–[14]. The bandpass (BP) filter [11], Hard- and Soft- thresholding filter [13], Serial filter [6], and Savitzky-Golay (SG) filter [12] have shown good SNR performance, while the total variation (TV) filter [14] and wavelet-based total variation (WATV) filter [10] have shown good RMSE results in the literature. In simulation and experimental studies, WATV-Wiener and the seven filters mentioned above are applied to both healthy lung sound signals and lung sound signals containing crackle and wheeze, and the performance is evaluated in terms of RMSE and SNR improvement. In comparison with the BP filter, Hard and Soft thresholding filter, Serial filter, SG filter, and TV filter in denoising noisy lung sound signals, the optimized WATV-Wiener technique achieved better RMSE results by 0.2–0.7 V in both simulation and experiment studies. In addition, compared to the seven filters as mentioned earlier, the WATV-Wiener achieved better SNR performance by 5–20 dB and 4–30 dB in simulation- and experimental-studies, respectively. Through the efficient parameters identified in our parameter tuning evaluation, WATV-Wiener filter achieved optimal RMSE results regardless of low of high noise variance in the lung sound signals — showing the capability in preserving signal characteristics from noise and further improving SNR.

This paper is organized as follows: Section II briefly describes the state of the art. This is followed by our data model and the assumption, and the problem formulation in Section III. Next, we present our proposed technique in Section IV. Section V presented the simulation results and discussions of WATV-Wiener filter parameters tuning, and denoising synthesized lung sound signals. We compared and discussed our simulation results with experimental results in Section VI, and the conclusion is presented in Section VII.

II. State of The Art

In the literature, adventitious lung sounds are indicators of lung dysfunctions, and they can be related to airway obstruction and various pulmonary diseases such as asthma, COPD, pneumonia, and sputum production [4], [15]. The adventitious lung sounds can be grouped as crackles and wheezes [4], [16]. Coarse crackles are noncontinuous, nonmusical, explosive, and have a typical frequency of 350–950 Hz and a duration of 10–15 ms. Contrarily, wheezes are continuous, musical, oscillatory, have a typical frequency range between 100 and 1000 Hz, and a duration of 100 ms. Hence, differentiating the adventitious lung sound signals from noise, as shown in Fig. 2, is critical for improving the lung function assessment.

The straightforward approach to mitigating external interference is linear high-pass or BP filtering with a specific cutoff frequency [11]. SG filter, a finite impulse response (FIR) filter, was proposed to denoise and smoothen the lung sound signal from noise [12]. An FIR-based filter, particularly the BP filter, can reduce unwanted noise in the low and high frequency ranges from the observed signal; however, the lung sound and noise interference may have spectral overlap in the low or the passband frequency range [3], [6], [17]. A combination of a chain of filters: FIR-based BP filter, a wavelet-based filter, and

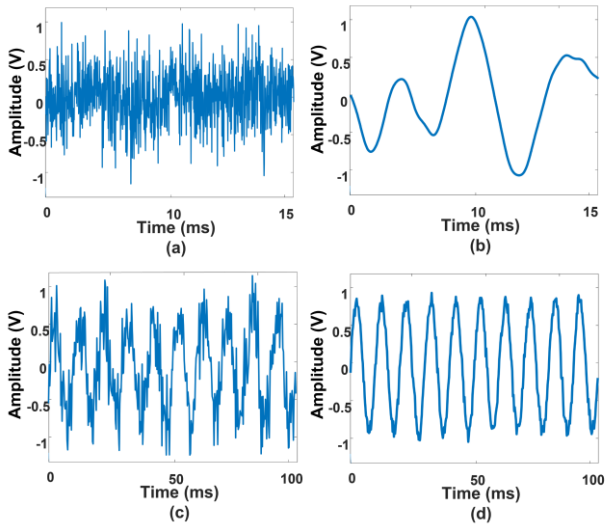

Fig. 2. Typical recorded lung sounds and the interesting waveform trend and characteristics for lung health assessment. (a) Noisy lung sounds recording with crackle; (b) Crackle waveform; (c) Noisy lung sound recording with wheeze, and (d) Wheeze waveform.

a least mean square adaptive filter was proposed (Serial) in [6] to overcome the problem in FIR-based filter in reducing unwanted noise from lung sound signals.

Classical wavelet-based universal soft thresholding (Soft), universal hard thresholding (Hard), or wavelet transform methods are a practical signal denoising approach when the actual noise-free signal is practically unknown [6], [13], [18]–[21]. Wavelet transform assumes the "nonstationary" region, typically lung sound, in the time domain produces significant wavelet transform coefficients (amplitude) over many wavelet scales. The "stationary" region, typically noise, decays quickly with increasing scale without affecting the signal quality. The limitation with classical wavelet transform is introducing artifacts such as spurious-Gibbs oscillations and noise spikes around discontinuities [9]. Generally, when the noisy wavelet coefficients exceed the threshold, noise spikes occur in the denoised signal [9]. When the noisy wavelet coefficients are less than the threshold and inaccurately set to zero causes the pseudo-Gibbs artifacts in the denoised signal [9]. TV denoising is introduced to improve the denoised signal by reducing the artifacts produced by wavelet transform [14]. However, TV denoising often produces undesirable staircase artifacts.

An alternative approach is to perform empirical Wiener filtering in the wavelet transform domain [22]. Since the actual signal is practically unknown as different individuals exhibit different adventitious lung sound characteristics, Wiener filtering becomes empirical [23]. Wavelet-based empirical Wiener filter considers both significant (signal) and insignificant (noise) wavelet coefficients for scaling/denoising. An acceptable signal estimate for Wiener filter construction is critical in the wavelet domain Wiener filtering [22]–[25]. The wavelet-domain empirical Wiener filtering uses two different wavelet transform bases (two/dual-stage transform): 1) Wavelet transform discards small coefficients (noise) and retains significant coefficients (signal) for denoising noisy signal. 2) Design of the empirical Wiener filter where the filter brings back insignificant coefficients (noise) for consideration and scales them by minimizing the mean square error (MSE) [22]–[25]. Sandeep et al. [22] showed that the empirical Wiener filter improved wavelet denoising and outperformed other thresholding denoising algorithms. Wavelet transform decorrelate signal and Wiener filter filtering of individual transform coefficients improved the signal estimate [22]–[25]. However, the limitation with wavelet-domain empirical Wiener filtering is that the approach requires two different wavelet transform bases. The effect on denoising the signals differs with different combinations of wavelet bases [22]–[25].

It was proposed in [9] a WATV filter approach to overcome the artifacts produced during denoising by modifying a single objective function. In addition, the WATV filter indirectly eliminates the need to select the appropriate wavelet transform bases required in the wavelet-based empirical Wiener filter. However, WATV still presents artifacts after denoising the signal, particularly in the lung sound signal containing crackle [10].

Inspired by [6], [9], [10], [22], a novel approach (WATV-Wiener) to denoising and filtering the noisy lung sound signals was proposed in this paper, which integrated WATV and the wavelet-based empirical Wiener filter effectively and uniquely. Firstly, WATV was synthesized and fine-tuned through case studies and was used to achieve a set of adequate denoised signal wavelet coefficients, and then the wavelet-based Wiener filter was designed to smooth the artifacts produced by the WATV denoising process. To the best of our knowledge, the combination and integration of WATV and the Wiener filter has not been investigated and reported in the literature [6], [9], [10], [22], particularly in the acoustic lung signal domain.

III. Numerical Modeling And Problem Formulation

Our lung sound model is based on the airflow transmission to the chest wall by the technique in the communication system and signal processing [26]–[28]. The lung sound model contains crackle and wheeze.

The lung sound is modeled as the flow source (airflow) hitting the airway [26]–[28]. When the airflow hits the airway, the lung sound is modulated by amplitude and frequency,

$$x_a(t) = x_s(t) m_a(t) m_f(t), \tag{1}$$

where $x_a(t)$ is the airflow hitting on the airway, $x_s(t)$ is the airflow; the amplitude and frequency modulation functions are denoted as $m_a(t)$ and $m_f(t)$, respectively.

The modulated airflow $x_a(t)$ is accompanied by noise $v_a(t)$ when it penetrates the airway wall, given as $x_f(t)$,

$$x_f(t) = x_a(t) + v_a(t), \tag{2}$$

The noise from the sensor was also transferred, as is customary when noise from electronic devices is fed into the recording system [26]–[28],

$$x(t) = x_f(t) + v_f(t), \tag{3}$$

where $x(t)$ is the airflow transmitted out of the chest wall or the modulated signal with noises, and $v_f(t)$ is the noise transferred from the sensor, such as an electronic stethoscope.

Noise is also produced by the ambient and other factors such as speech and cough during the lung sound recording,

$$y(t) = x(t) + v_e(t), \tag{4}$$

where $y(t)$ is the airflow that is captured by the sensor with noise, and $v_e(t)$ is the noise caused by ambient. Substituting (1)–(3) into (4), we will have our received lung sound

containing noise,

$$y(t) = x_s(t)m_a(t)m_f(t) + v_a(t) + v_f(t) + v_e(t). \quad (5)$$

A reasonable assumption is that the noises are a zero-mean process having a probability density distribution that can be defined with mean and variance, uncorrelated with the transmitted lung sound $x(t)$, with varying SNR levels, similar to those classical signal denoising studies [9], [18], [24], [25]. Hence, we modeled the noises as white Gaussian noise (WGN) [7], [10] and combined $v_a(t)$, $v_f(t)$, and $v_e(t)$. Therefore, (5) can be simplified to (6) similar to a linear system, where $y(t)$ is the received lung sound signal (output) containing WGN (error) $v(t)$ and the desired lung sound signal (input) $x_a(t)$ as in (1),

$$y(t) = x_a(t) + v(t). \quad (6)$$

From (6), the desired signal $x_a(t)$ is contaminated by noise $v(t)$ from the collisions of the airflow onto the airway, electronic devices, and ambient noise; thus, we have to remove the noise from the captured lung sound signal $y(t)$ through denoising. However, an inappropriate denoising method may introduce artifacts, particularly in the lung sound signal domain [10], which may lead to misinterpretation and affect the assessment. Thus, the design of an optimal lung sound denoising technique is crucial for an accurate assessment [5], [29], [30].

IV. WATV-Wiener Denoising Filter

A good denoised signal is achieved in [9], [10] (low RMSE); however, defects such as the staircase effect still exist after denoising noisy lung sound signals [10], hence; we proposed the integration of the WATV-Wiener filtering technique to reduce ambient noise and smoothen the denoised signal further to achieve a better-denoised signal with higher SNR and insensitive to both high and low noise variance while maintaining the optimal RMSE performance.

The principle of the integrated filter is discussed in this section, starting with the synthesis of the WATV filter in Section IV-A, whereby the indirect approach of parameter tuning and selection will be discussed in Section V-B, followed by the design of the empirical Wiener filter in Section IV-B. Lastly, the customized filter algorithm and block diagram are presented in Section IV-C.

A. Wavelet Threshold Total Variation Denoising

We first perform wavelet transform W to (6) to achieve (7) [9], where n is denoted as the sample index, and the total number of samples N over a known time T is defined as $N = F_s T$, where F_s is the sampling frequency in this work,

$$\mathrm{W}y(n) = \mathrm{W}x_a(n) + \mathrm{W}v(n),\ n = 1, 2, \ldots N. \quad (7)$$

Equation (7) contains the entire signal coefficients $\mathrm{W}y(n)$ that contains dependable signal coefficients $\mathrm{W}x_a(n)$ and ambiguous signal coefficients $\mathrm{W}v(n)$. To accurately estimate the dependable signal coefficients from the signal coefficients $\mathrm{W}y(n)$ in (7), a 5-scale undecimated discrete wavelet transform W with two vanishing moments fulfilling the Parseval frame condition, and Daubechies filter (due to its translation-invariant property in denoising) with a low- and high-pass analysis filter was designed and applied onto the signal for denoising [9]. The 'nonstationary' region of the lung sound signal produces significant wavelet transform coefficients (amplitude) over many wavelet scales. Most of the significant coefficients at each wavelet scale correspond to the desired lung sound signals, whereas the insignificant wavelet coefficients with small values, typically noise, are shrunk during denoising. ω is denoted as the wavelet coefficients containing our signal x_t required for designing the empirical Wiener filter [9], [22],

$$\omega = \mathrm{W}x_t. \quad (8)$$

Thus, the estimation of signal x_t denoted as $\hat{x}_t$ can be obtained by inverse wavelet transform W^{-1} of wavelet coefficients ω once the estimated wavelet coefficients $\hat{\omega}$ is available [9],

$$\hat{x}_t = \mathrm{W}^{-1}\hat{\omega}. \quad (9)$$

The wavelet coefficients $\hat{\omega}$ in (9) can be identified in the following way. 1) Split augmented Lagrangian shrinkage algorithm (SALSA) [14], [17] is applied to compute the wavelet coefficient in (10) with the condition that the wavelet coefficient between $1/2\,\|\mathrm{W}y - \omega\|_2^2 + \sum_{j,k}\lambda_j\phi(\omega_{j,k};\alpha_j)$ and $\beta\|D\mathrm{W}^{-1}\omega\|_1$ are equal. 2) To achieve a balance between wavelet transform and TV denoising, they are controlled by a control parameter $0 < \eta < 1$ [9], [10]. The regularization parameter λ_j and TV parts β from (10), where σ is related to the WGN variance σ^2 in each wavelet scale j, is presented in (11) and (12), respectively [14]. From the regularization parameter λ_j above, the threshold shape controller is identified as $\alpha_j = 1/\lambda_j$.

$$\hat{\omega}(n) = \arg\min_{\omega}\left\{F(\omega) = \frac{1}{2}\|\mathrm{W}y - \omega\|_2^2 + \sum_{j,k}\lambda_j\phi(\omega_{j,k};\alpha_j) + \beta\left\|D\mathrm{W}^{-1}\omega\right\|_1\right\}. \quad (10)$$

$$\lambda_j = 2.5\eta\sigma/2^{j/2} \quad (11)$$

$$\beta = (1-\eta)\left(\sqrt{N}\right)/4\sigma \quad (12)$$

The indexed terms j and k are used to represent the scale and vanishing moment of the signal in the wavelet coefficients $\omega_{j,k}$ respectively. The $\left\|D\mathrm{W}^{-1}\omega\right\|_1$ can be defined as the total variation of signal estimation, where D is the first-order difference matrix. The single indexed normalized wavelet coefficient is represented as, e.g., $\|x\|_1 = \sum_n|x_n|$, $\|x\|_2 = \sum_n|x_n|^2$. Doubly indexed normalized wavelet coefficient is denoted as, e.g., $\|\omega\|_2^2 = \sum_{j,k}|\omega_{j,k}|^2$.

B. Modified Empirical Wiener Filter

The obtained signal $\hat{x}_t$ is the estimated signal of wavelet filter containing the lung sound of interest and dubious signal such as artifacts. The estimated reference signal $\hat{x}_a$ which is linearly related with $\hat{x}_t$, as shown in (13).

$$\hat{x}_a = \mathrm{W}^{-1}H\mathrm{W}\hat{x}_t, \quad (13)$$

The Wiener filter is designed to smooth the pilot estimation $\hat{\omega}$ in (10) to predict the remaining dubious coefficients; thus,

the design of the Wiener filter in (14) estimates the entire signal coefficients consisting of both trustworthy and dubious coefficients,

$$H(n)=\frac{\hat{\omega}^2(n)}{\hat{\omega}^2(n)+\sigma^2}. \quad (14)$$

The coefficients estimate from (10) guarantees that the Wiener filter in (14) can further smooth the trustworthy coefficients in the pilot estimate of the wavelet coefficient $\hat{\omega}$ (10) through the bias of the Wiener filter. Smoothing occurs when the wavelet coefficients $\hat{\omega}$ are larger than the noise variance σ^2. However, if the pilot estimate $\hat{\omega}$ is small or similar to the noise variance σ^2, the denoised signal has biases, leading to a significant gain ($H < 1$) in the MSE sense. Thus, we can identify if the denoised wavelet coefficient is overly stretched with the Wiener filter by comparing WATV-Wiener and WATV RMSE results.

The estimated denoised wavelet coefficients $\hat{\omega}$ is applied to empirical Wiener filter design in (13)–(14) for smoothing and mitigating the artifacts by minimizing the RMSE to design an improved weighting profile in (14) [22].

C. WATV-Wiener Denoising Algorithm

Inspired by [9], [22], a unified wavelet threshold denoising filter (WATV) is first customized to reduce the interference noise, achieving an adequate denoised signal coefficient from the lung sounds by estimating all wavelet coefficients (reliable and unreliable) concurrently. The estimated signal coefficient is fed into the empirical Wiener filter for smoothing by minimizing the denoised signal overall mean square error in the process of inverse filtering. WATV denoising strategy estimates all wavelet coefficients in (7) concurrently by computing the optimal single objective function in (10) to provide an estimate of x_a, denoted as x_t in (8) with the underlying understanding that dependable signal coefficients will survive thresholding and zeros most of the ambiguous signal coefficients. We denote $\hat{x}_t$ as the pilot estimate related via (8) and (9) with the fundamental explanation that $\hat{x}_t$ contains estimates of dependable signal coefficients $\hat{\omega}$ and the modified empirical Wiener filter in (13) smooths $\hat{x}_t$ from artifacts output from the WATV filter. The signal coefficient $\hat{\omega}$ is treated as approximate maximum posteriori estimation of variance to design an empirical Wiener filter H in (14) to smooth the remaining ambiguous signal coefficients from $\hat{\omega}$ which resulted from the artifacts produced from WATV denoising strategy, and thus output an estimated desired signal $\hat{x}_a(n)$ through the signal coefficient $\hat{\omega}$ [9], [10], [22]–[24]. The proposed technique is summarized in Fig. 3.

From Fig. 3 and (7)–(14), we applied the estimated denoised signal $\hat{x}_t$ from WATV to obtain an adequate signal coefficients estimate $\hat{\omega}$ instead of deciding on two wavelet transform bases to obtain an optimal empirical Wiener filter [9], [10], [22]–[24]. The Wiener filter further reduces the ambiguous signal coefficient that produces artifacts from the WATV. The approach has been simplified into a linear system instead of the dual wavelet transform and smooths the signal through the additional empirical Wiener filter. The pseudocode of the proposed WATV-Wiener algorithm is shown in Fig. 4.

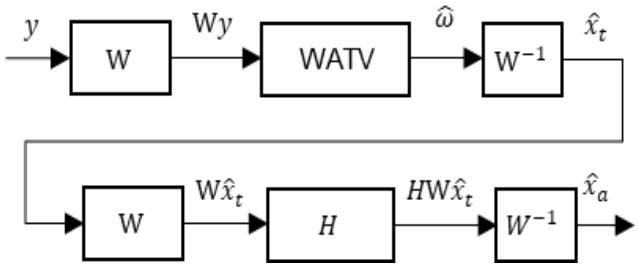

Fig. 3. A hybrid technique of WATV and wavelet-based empirical Wiener filtering.

V. Lung Sound Modeling And Simulation

The modeling of both healthy and adventitious lung sound signals x_s shown in (1) is expressed in Section V-A [26]–[28], followed by the optimization and evaluation of filter parameters affecting the overall proposed filter performance in the SNR sense, which were demonstrated in Section V-B. In Section V-C, the simulated noisy lung sound signals shown in Fig. 5 were fed into the optimized WATV-Wiener filter and seven other state-of-the-art filters that had shown good SNR or RMSE results in the literature for denoising and performance comparison in terms of SNR and RMSE [6], [9]–[14]. The sampling frequency is set to F_s = 4000 Hz in this work, and we

//Input: Noisy data (y); Number of vanishing moment (k); Regularization parameter (λ_j); TV parts (β); Step size (μ); Number of wavelet scale (j); Number of iterations ($niter$), Threshold function (θ)
//Variables: Wavelet transform (W); Wavelet coefficient (ω)
//Initialization
$\omega = \mathrm{W}y$;
//Identifying wavelet coefficient in (10) by iteratively minimizing with respect to ω and u with variable splitting and augmented Lagrangian approach.
$u = \omega$; $d = \omega$; $c = 0$;
//Iteration till convergence between $\boldsymbol{\omega}$ and $\boldsymbol{u}$.
For i = 1:$niter$
$p_{j,k} = [\mathrm{W}y + \mu(u - d)]/(1 + \mu)$
//Finding the wavelet coefficient ω for all j, k with the input from θ, p, λ_j, μ, $a_j = 1/\lambda_j$
$\omega_{j,k} = \theta\left(p_{j,k};\ \lambda_j/(1+\mu);\ a_j\right)$
$c = d + \omega$
//Total variation denoising (tvd) requires data input from c, length of the data input (N) and TV parts
$d = \mathrm{W}[\mathrm{W}^{-1}v - tvd(W^{-1}c; N; \beta/\mu)]$
$u = c - d$
$d = d - (u - \omega)$
end For
Preliminary Output: Denoised wavelet coefficient ($\hat{\omega}$), where signal $\hat{x}_t = \mathrm{W}^{-1}\hat{\omega}$
//Empirical Wiener filter design for smoothing: H
$H = \hat{\omega}^2/(\hat{\omega}^2 + \sigma^2)$
//Smooth denoised output
$\hat{x}_a = \mathrm{W}^{-1}H\mathrm{W}\hat{x}_t$

Fig. 4. WATV-Wiener algorithm.

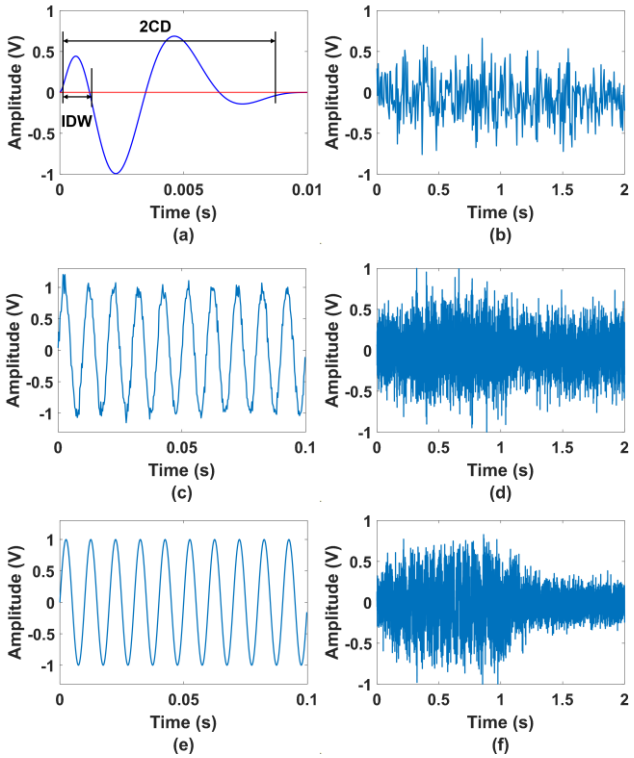

Fig. 5. Simulated lung sound signals transmitted out of the chest wall, corrupted with additive WGN as the noise component v(t). (a) Simulated airflow source crackle; (b) Lung sound signal containing crackle transmitted onto chest wall with additive WGN; (c) Simulated airflow source wheeze; (d) Lung sound signal containing wheeze transmitted onto chest wall with additive WGN; (e) Simulated healthy lung sound; and (f) Healthy lung sound signals are transmitted onto the chest wall with additive WGN

performed 500 simulation runs on denoising lung sound signals at each noise level. Analyses were performed offline through MATLAB R2019b in our simulation studies.

RMSE and SNR were utilized as performance metrics after denoising the observed lung sound signal y in (6). We determined RMSE by employing the amplitude of denoised and noise-free signals and expressing the differences in root mean square sense shown in (15). We defined SNR by finding the ratio of denoised signal peak amplitude to noise peak amplitude and expressed the ratio using the logarithmic decibel scale in (16),

$$\text{RMSE} = \sqrt{\text{mean}\left[\left(d-x\right)^2\right]}, \tag{15}$$

$$\text{SNR}=20\left[\log\left(\frac{d}{y-x}\right)\right], \tag{16}$$

where x is the noise-free simulated signal, y is the simulated noisy signal, and d is the denoised signal.

A. Synthesis of Lung Sound with Crackle and Wheeze, and Healthy Lung Sound

To obtain both adventitious and healthy lung sound shown in (1) and depicted in Fig. 5(a), Fig. 5(c), and Fig. 5(e), airflow source $x_s(n)$ is first modulated by the frequency modulation m_f cosine wave in (17) with an amplitude of 1 V, and frequency of F = 400 Hz, followed by the amplitude modulation m_a sawtooth wave in (18) with an amplitude of 1 V amplitude, and frequency of F = 400 Hz [26], [27]. The noise v from (2)–(6) and shown in Fig. 5(b), Fig. 5(d), and Fig. 5(f) is presented last in this Section V-A.

$$m_f(n)=\cos\left(2\pi\left(F/F_s\right)n\right), \tag{17}$$

$$m_a(n)=\frac{1}{2}-\frac{1}{\pi}\sum_{k=1}^{5}\frac{1}{k}\sin\left(k\pi\frac{F}{F_s}n\right), \tag{18}$$

where k is the order of harmonics of amplitude modulation.

Employing the equations proposed in [31], we simulate adventitious airflow (crackle) transmitted to the airway using (19)–(20). We present the crackling signal x_s(n) as two periods, and the crackle modulation function in (20) is employed to shift the energy of x_s(n) to the initial part of the shape. Fig. 5(a) presented the simulated crackle, with initial deflection width (IDW) = 1.2 ms and two cycle duration (2CD) = 9.8 ms [20],

$$x_s(n)=\left[\sin\left(4\pi n^{\alpha}\right)\right]m_c(n),\ \alpha=\frac{\log(0.25)}{\log(0.12)}, \tag{19}$$

$$m_c(n)=0.5\left\{1+\cos\left[2\pi\left(n^{0.5}-0.5\right)\right]\right\}. \tag{20}$$

Synthesis of wheeze as airflow source $x_s(n)$ [28] and then transmitted to the airway $x_a(n)$ is presented in (21). The airflow source $x_s(n)$ for wheeze was simulated as a pure sine wave with 1 V amplitude, F = 100 Hz, and WGN at 50 µW [28] The simulated wheeze is presented in Fig. 5(c),

$$x_s(n)=\sin\left(2\pi\left(F/F_s\right)n\right)+v_w(n), \tag{21}$$

where $v_w(n)$ is the WGN for wheeze airflow source.

The synthesis of healthy lung sound signals is shown in (22) [28], similar to wheeze in (21) except for the insertion of WGN and presented in the simulated healthy lung sound in Fig. 5(e).

$$x_s(n)=\sin\left(2\pi\left(F/F_s\right)n\right), \tag{22}$$

The modulation's accompanying noises $v_a(n)$ were inserted into the acoustic signals in (19), (21), and (22) that penetrate to the airwall shown in (2), with WGN power level and SNR at 0.6 dBm and 0.01 dB [28], respectively. The parameters chosen demonstrated that the proposed communication model corresponds with the physiological characteristics of the actual lung sounds [28]. Finally, the microphone received sound combined with the WGN $v_f(n)$, power at 10^{-6} dBm, as is usually the case in electronic communication [26]–[28]. From the above noise parameters, in an uncontrolled environment, the electronic noise $v_f(n)$ is dominated by the noise produced internally by the airway wall and ambient interference. However, in a quiet and controlled environment, situation of the electronic noise may have different impact on the simulation studies. Thus, we included the noise power in our simulation studies, consistent with the literature simulation studies [26]–[28].

We generated WGN at various SNRs and were employed as the noise component $v(t)$ in (6), similar to the literature [10], [28]. We varied the SNR values between 0 dB and 20 dB with a 2 dB increment rate resulting in 11 noise levels. We superimposed each noise level on the individual simulated lung sound signals, which gave us the observed physiological signals $y(t)$ in (6) and presented in Fig. 5(b), Fig. 5(d), and Fig. 5(f), with a specific SNR. From Fig. 5, we can observe the similarity between our simulated signal and the actual noisy signal

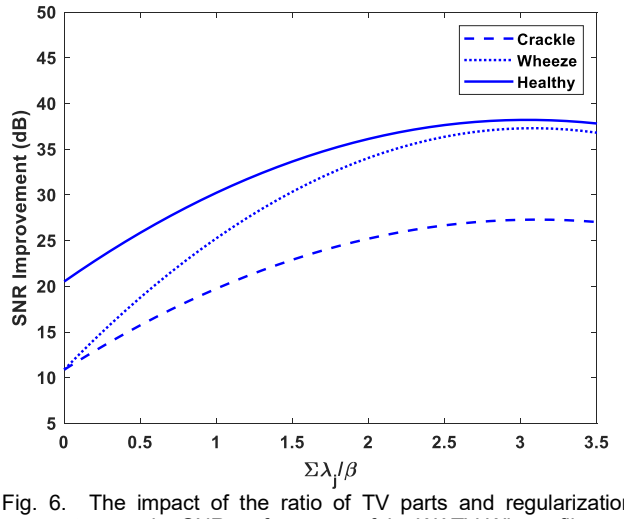

Fig. 6. The impact of the ratio of TV parts and regularization parameters on the SNR performance of the WATV-Wiener filter.

captured in an uncontrolled environment with an electronic stethoscope and microphones in the literature [6], [18].

B. Tuning of Parameters for Optimizing the WATV-Wiener Filter

The simulations were tailored to optimize the overall filter performance by modifying three parameters η, σ, and N that influence the TV parts β and regularization parameter λ_j from (10)–(12). We can observe in (10) that both β and λ control the pilot estimation of the denoised wavelet coefficients in our proposed technique. As the pilot estimation affects the designing of the empirical Wiener filter and the overall filter performance; hence, the pilot estimation of the denoised wavelet coefficients is critical. The parameter η estimates were available in the literature; however, no case studies on how the parameter adjustment affects the filter performance, particularly in the lung sound signal domain, were attempted or discussed [9], [10]. Additionally, the literature has not discussed the filter's SNR performance in recovering signals of interest from noisy lung sound signals [9], [10]. Thus, to evaluate the effect of the parameter η on the overall filter, we will be comparing the performance of the denoised noisy lung

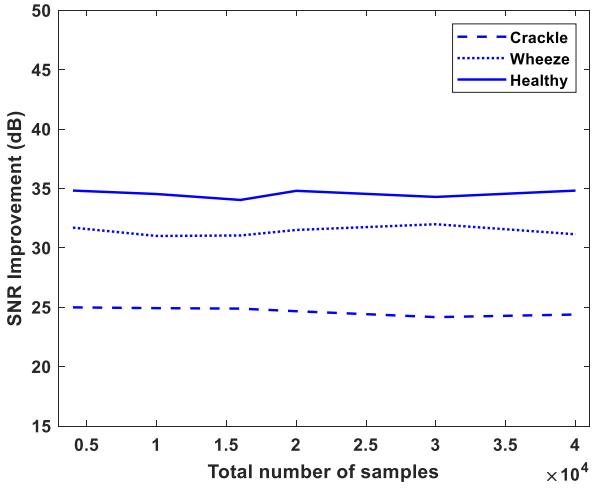

Fig. 7. The impact of baseline parameter η = 0.90 on the various total number of samples N in terms of the denoising SNR performance.

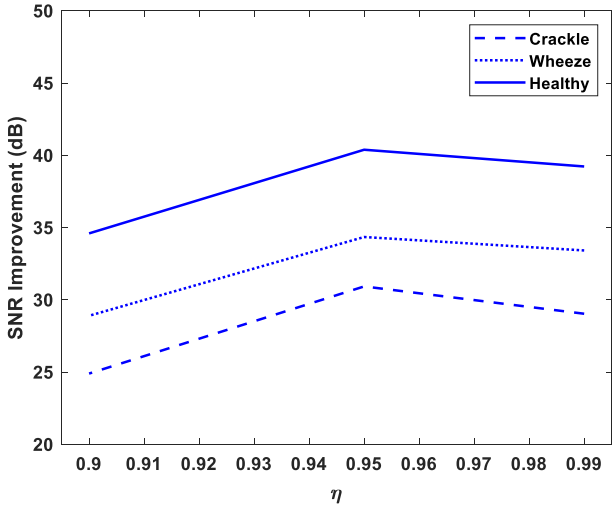

Fig. 8. The impact of parameter η on the WATV-Wiener filter denoising SNR performance.

sound signals in the SNR sense.

In our initial investigation into optimizing SNR performance, three possible simulation case studies were evaluated through adjusting η, while keeping σ = 10 and the total number of samples N = 4000. In the first demonstration, we kept $0.76 < \eta < 1$, e.g., $\eta = 0.80$, $\eta = 0.90$, which resulted in $\sum\lambda_j > \beta$. Next, we adjusted $0 < \eta < 0.76$ to a lower value, e.g., $\eta = 0.2$, $\eta = 0.5$, resulting in $\beta > \sum\lambda_j$. Lastly, we balanced both $\beta \approx \lambda_j$ with η = 0.76. The mean SNR improvement with respect to the ratio between TV parts and regularization parameter in the three explored scenarios were demonstrated in Fig. 6. We can observe that the SNR performance of the filter is at the lowest when $\beta > \sum\lambda_j$, with a ratio < 1, and achieved the best SNR performance when $\sum\lambda_j = 3\beta$, at η = 0.90.

We have identified that the condition η = 0.90 as a baseline for optimizing the SNR performance from the results in Fig. 6. An additional observation from the TV parts β in (12) and the regularization parameter λ_j in (11) wherein they were also determined by the total number of sample N. Typical lung sound signals comprised of minimally two respiratory cycles with time $T \approx 4$ s, F_s = 4000 Hz in the literature [3], [18], [28].

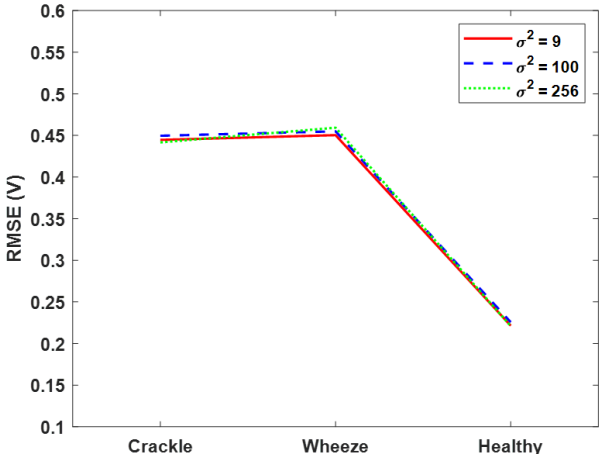

Fig. 9. Average RMSE of denoised lung sound signals with various noise variance in the lung sound signals.

Hence, we have adjusted the total number of samples N to our lung sound signals to determine if N affects the overall filter performances. We presented the mean SNR performance with respect to N with the parameters in our initial investigation, e.g., $\eta = 0.90$, $\sum \lambda_j \,/\, \beta = 3$ in Fig. 7.

The performance of the WATV-Wiener filter was not affected by the total number of samples presented in Fig. 7 in terms of SNR performance compared to Fig. 6 and showed a similar SNR performance trend at the ratio $\sum \lambda_j = 3\beta$, with η = 0.90 regardless of number of signal samples.

As the parameter η range between 0 and 1, we have identified $0.9 < \eta < 1$ as a baseline parameter from Fig. 6 and Fig. 7 discussion above. The remaining question is, what is the optimal parameter range in η for our filter? Thus, to present the optimizing of parameter η from the baseline parameters identified from our case studies, we set different possible combinations of parameter η, e.g., $\eta = 0.90$, $\eta = 0.95$, and η = 0.99 to evaluate the optimal SNR performance of our overall filter on different noisy lung sound signals and presented the result in Fig. 8. An optimal SNR parameter is achieved, as observed from Fig. 8. WATV-Wiener filter obtained higher improved SNR by 3–8 dB with $\eta = 0.95$ compared to the literature [9], [10] estimated parameter, and our initial investigation $\eta = 0.90$, and the SNR performance is similar for both $\eta = 0.95$ and $\eta = 0.99$, with a variation of 1 dB. In addition, WATV-Wiener performed better in terms of SNR with the single setting of $\sum \lambda_j > \beta$ with $0.95 \leq \eta < 1$ compared to the other case settings shown in Fig. 6–Fig. 8.

From the case studies, optimal SNR results were obtained in Fig. 6–Fig. 8; we recommend the following optimized parameters for denoising typical lung sound signals by tuning $\sum \lambda_j = 3\beta$ with $0.95 \leq \eta < 1$.

Ultimately, the denoised signal ought to retain waveform characteristics of interest without overly deforming the lung sound signals. Thus, we set the ideal parameter $0.95 \leq \eta < 1$ to denoise noisy lung sound signals with different noise variances and presented the RMSE result in Fig. 9. Our filter achieved consistent RMSE results with different noise variance in the system in Fig. 9, showing robustness to the noise variance.

C. WATV-Wiener Filter Fine-tuned Parameters Performance Evaluation and Discussion

Optimal quantitative findings such as SNR of certain prior denoising approaches may seem promising, but the inappropriate selection of parameters, e.g., in the wavelet thresholding, may result in a high SNR, albeit evident artifacts are introduced in the signal processing. Thus, RMSE is essential in identifying that the denoising filter retains the frequencies of interest and waveform characteristics. In the literature, WATV is an optimal denoising filter in the RMSE sense [9], [10], [32]. Our goal is to denoise the signal without affecting the waveform characteristics while improving the SNR; thus, with the parameters identified in the optimal tuning study, $0.95 \leq \eta < 1$, we compared the WATV-Wiener filter with other established lung sound signal filters in the literature [6], [9]–[14] and presented the mean RMSE and SNR results in Fig. 10(a)–Fig. 10(c), and Fig. 10(d)–Fig. 10(f), respectively. The simulated lung sound signals have the following parameters: noise variance $\sigma^2 = 9$, $F_s = 4000$ Hz, and the total number of samples N=16000.

We can observe WATV denoising filter is optimal in terms of RMSE from Fig. 10(a)–Fig. 10(c), achieving mean RMSE of 0.43 V, 0.47 V, 0.21 V in adventitious lung sound signals containing crackle and wheeze, and healthy lung sound signals,

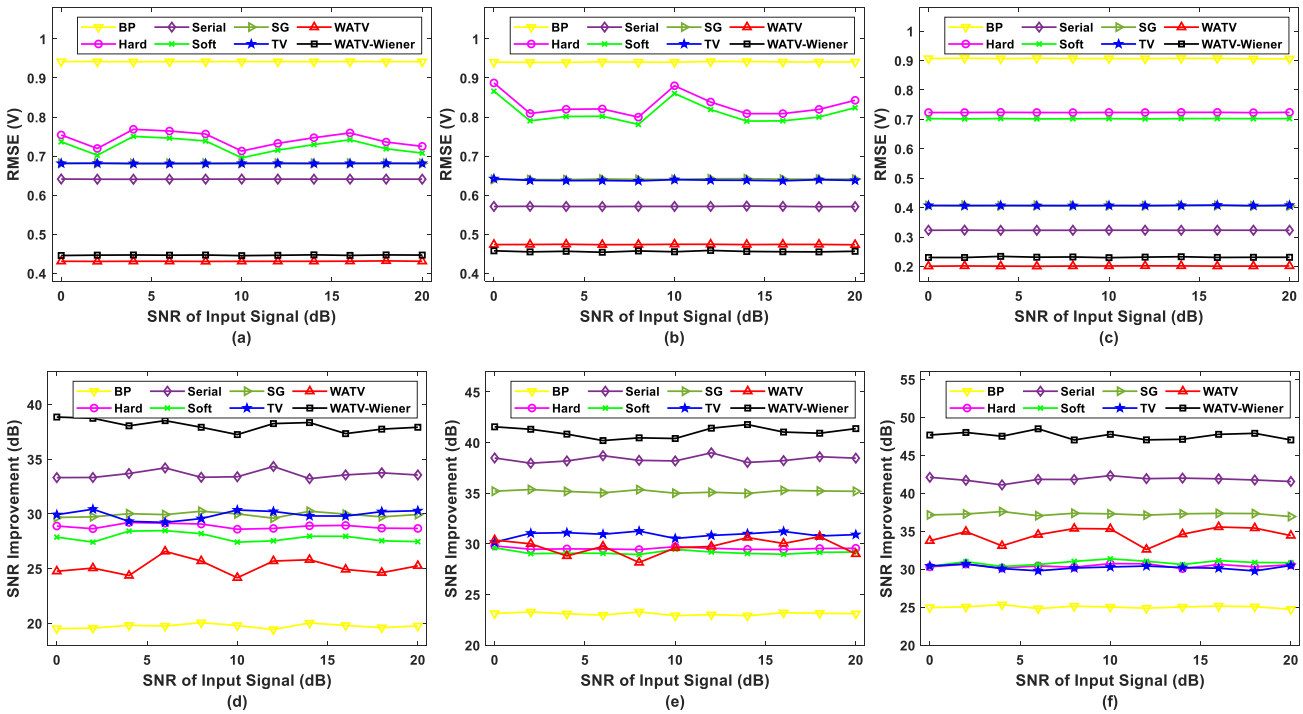

Fig. 10. Average RMSE (a)-(c) and SNR improvement (d)-(f) of denoised healthy and adventitious lung sound signals to various SNR values of the input signal. (a), (d) Lung sound signal containing crackle; (b), (e) Lung sound signal containing wheeze; and (c), (f) Healthy lung sound signal.

respectively, consistent with the findings in the literature [9], [10], [32]. WATV-Wiener shadows WATV sharply, within ±0.02 V, or within 10% in the absolute relative change in terms of optimal RMSE, and performed better by 0.2–0.7 V compared to remaining filters, i.e., BP, Soft, Hard, Serial, and TV. From Fig. 10(d)–Fig. 10(f), WATV-Wiener obtained the best mean improved SNR of 38.09 ± 0.80 dB, 41.03 ± 0.79 dB, 47.56 ±0.73 dB in crackle, wheeze, and healthy lung sound signals, respectively. From the results in SNR and RMSE, the BP filter has the lowest SNR performance and worse RMSE results; the reason could be due to denoised lung sound signals containing overlapping noise spectral. The finding in RMSE is consistent with the literature where a single linear infinite impulse response or FIR-based filter may not be sufficient to denoise a noisy signal, and the noise affects the waveform characteristics [11], [18].

From the SNR and RMSE results in Fig. 10, WATV-Winer filter can achieve optimal RMSE results similar to the optimal RMSE-sense WATV, and further achieved higher noise removal in terms of SNR by another 5–20 dB compared to other established lung sound signals filters. From the RMSE and SNR results, WATV-Wiener showed it could retain waveform characteristics (low RMSE) while improving SNR from denoising various inputs of SNR lung sound signals, showing robustness to severe noise. The WATV-Wiener performance benefits achieved could be due to the optimized pilot estimation of the wavelet coefficient $\hat{\omega}$ and smooth the pilot denoised wavelet coefficient with the complementing diagonal weighting matrix H from the empirical Wiener filter. As shown in Fig. 8–Fig. 10, without the optimal parameters in the pilot estimation of the denoised wavelet coefficient, the integration of the WATV filter and empirical Wiener filter may not have achieved optimal denoised lung sound SNR performance. WATV estimates the wavelet coefficients $\hat{\omega}$ by considering both insignificant (noise) and significant (signal) coefficients, we used the estimated signal estimates from WATV to design an empirical Wiener filter H to smooth and reduce the artifacts on the denoised signal. The empirical Wiener filter scales the coefficients by minimizing the MSE to design an improved weighting profile $H \approx 1$, with a WATV coefficient more significant than the noise variance, $\hat{\omega}^2 \gg \sigma^2$. Thus, pilot estimation of the denoised wavelet is critical to improving our filter's weighting profile. Our proposed hybrid technique can decrease the denoised signal's bias and achieve an optimal filter in SNR performance. Under the condition of the noise variance σ^2 is greater than the estimated denoised signal $\hat{\omega}^2$, the weighting profile will contribute to the gain in wavelet coefficient resulting in a lower SNR performance.

VI. Experimental Studies

To ensure the denoising performance stability of the WATV-Wiener filter between our simulation studies and actual respiratory sound, we quantitatively compare the WATV-Wiener filter and other prominent filters in the literature, similarly to our simulation studies, in the denoising experiment studies [6], [9]–[14].

We shortlisted healthy volunteers in our experimental studies with their verbal consent and no history of respiratory diseases in the past 1 month. We collected 10 healthy lung sound signals from our volunteers with our system presented in Section V-A. and evaluated the system SNR performance compared against a commercial product used for capturing lung sound signals. We experimented in an uncontrolled environment with an average 59 ± 0.54 dBA sound pressure level, similar to a hospital noisy intensive care unit, where emergency alarm, communications, and critical care are often happening [33].

Due to the current pandemic situation globally, we could not get actual respiratory patients for the experiment. Hence, 17, 10, and 13 unhealthy lung sound signals containing crackle, wheeze, or both crackle and wheeze (mixed) were shortlisted from an open-access respiratory database [34], respectively. The respiratory database [34] contained adventitious lung sound signals (crackle, wheeze) from volunteers diagnosed with COPD, asthma, and respiratory tract infection. The respiratory database [34] captured volunteers' respiratory sounds by digital stethoscope or an array of MEMS microphones in a clinical or home setting, with qualified independent reviewers annotating the signals. The signals also contain cough, speech, and throat clearing. The shortlisted respiratory signals have a minimum sampling frequency of F_s = 4000 Hz, and a minimum recording time of T = 10 s. A total of 50 recordings from our captured healthy lung sound signals and the shortlisted respiratory signals are passed through the denoising filters to estimate the denoised signal's SNR output.

Before denoising, a bandpass filter ranging from 150 Hz–1300 Hz has been applied to remove other major artifact events such as cough and throat clearing. All patients in the respiratory signal database had COPD with comorbidities – heart failure. Hence, signals below 150 Hz are excluded. We chose a maximum of 1300 Hz as the upper bandpass limit in our paper as F_s = 4000 Hz to avoid aliasing effects. In the literature, healthy, wheeze, and crackle frequency signal falls within our bandpass range of 150 Hz and 1300 Hz [3]–[5], [28]; thus, it should be sufficient to retain the interest frequency range and adventitious lung sound characteristics after denoising.

The estimated noise variance [35] is about σ^2 = 0.05 (σ = 0.23) from our healthy lung sound signal measurement in our experimental studies. We resampled the lung sound signals with a sampling frequency of F_s = 4000 Hz, and applied σ = 0.23, and the optimal parameter evaluated from our simulation studies, η = 0.95 to our experiment analysis as the sound pressure level for capturing our healthy lung sound signals and the database is similar. The static and ambient noise in the database may be different from our captured lung sound signals; however, we have also demonstrated earlier that the WATV-Wiener filter is insensitive to noise variance in our simulation studies, achieving similar SNR and RMSE performance in both low and high noise variance with $0.95 \le \eta < 1$.

We present the computation of RMSE for our captured lung sound signals in (23), the SNR for our captured lung sound signals, and the database in (25) and (26), respectively,

$$\mathrm{RMSE}_{\mathrm{system}} = \sqrt{\mathrm{mean}\left[\left(d-x\right)^2\right]}, \tag{23}$$

where d denotes the amplitude of denoised lung sound signals, x represents the amplitude of noise-free lung sound signals given in (24),

$$x = a_s - a_n, \tag{24}$$

where the captured lung sound signals with noise and captured ambient noise without lung sound signals are denoted as a_s and

a_n, respectively.

The computation of SNR in (25) and (26) is similar to (16), defining SNR by finding the ratio of denoised signal peak amplitude to noise peak amplitude and expressing the ratio using the logarithmic decibel scale.

$$\mathrm{SNR}_{\mathrm{system}} = 20\left[\log 10\left(\frac{d}{a_n}\right)\right], \tag{25}$$

where a_n is the noise peak amplitude from our system electronic static noise and ambient noise without lung sound signals, and d denotes the filter denoised signal peak amplitude.

There is a slight modification for the computation of database SNR in (26) as noise is unavailable; thus, 'noise' is defined as subtracting the denoised signal from the noisy signal,

$$\mathrm{SNR}_{\mathrm{database}} = 20\left[\log 10\left(\frac{d}{f_y - d}\right)\right], \tag{26}$$

where, f_y is the noisy signal peak amplitude from the database, and d is the denoised signal peak amplitude.

A. Acoustic Signal Acquisition

The motivation to assemble an acoustic sensor-based MEMS for capturing lung sounds is that a MEMS sensor is cheaper, a few dollars per piece compared to an electronic stethoscope, hundreds of dollars, particularly when an array of sensors is required to capture the acoustic signals. The research team assembled the system shown in Fig. 11 to record the lung sound signals, and the design specifications are similar to the literature [1]–[3], [33], [36]. The primary module of the equipment is a high SNR microelectromechanical system (MEMS) microphone with a frequency response between 50 Hz and 20 kHz. The sampling frequency of the MEMS microphone is 44100 Hz, and the MEMS sensor consists of a signal conditioning function, an analog-to-digital converter, decimation and anti-aliasing filters, power management, and an industry-standard 24-bit time-division multiplexing interface.

3M electronic stethoscope has 'proprietary' ambient noise reduction technology that eliminates an estimated 85% of ambient background noise interference without eliminating critical lung sounds. Therefore, we benchmark our system performance against a 3M electronic stethoscope. The SNR computation for our system and 3M electronic stethoscope can be expressed as $\mathrm{SNR} = 20\log(\bar{a}_s/\bar{a}_n)$, where, $\bar{a}_s = \sum(a_s - a_n)/\mathrm{N}$ represents the mean peak amplitude of the signal, and $\bar{a}_n = \sum a_n/\mathrm{N}$ is the mean peak value of the collected noise without lung sound signal from our MEMs sensor and 3M electronic stethoscope. a_s is the peak amplitude of the collected lung sound signal with noise, a_n is the peak value of the collected noise without lung sound signal, and $\mathrm{N} = 10$ is the number of collected signals. We obtained an estimated SNR of 71.63 dB and 68.73 dB from our system and 3M electronic stethoscope, respectively. Our sensor device can perform similarly to a commercial 3M electronic stethoscope in terms of SNR.

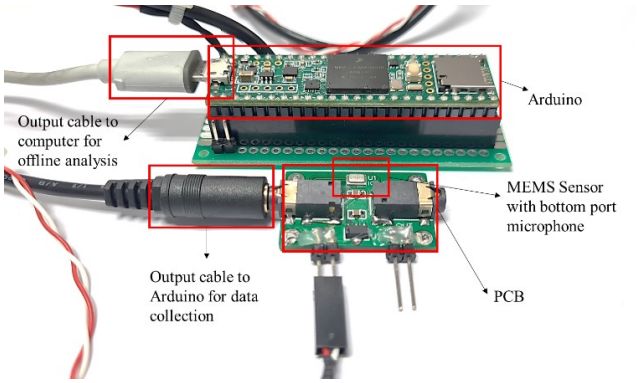

Fig. 11. Lung sound signal recording equipment.

B. Experiment Results and Discussion

We summarized the denoised experimental lung sound signals RMSE and SNR in Fig. 12 and Fig. 13, respectively. From Fig. 12, WATV-Wiener achieved a similar optimal RMSE of 0.1933 V compared to the optimal WATV filter in the RMSE sense at 0.1938 V, achieving an absolute relative change of about 0.26%. In addition, we can observe a similar trend from our simulation studies, particularly in the BP filter, where noise presence in the overlapped spectral may affect the overall filter signal quality, resulting in a high RMSE result of 0.99 V. Altogether, the WATV-Wiener filter achieved better and optimal RMSE results by about 0.1–0.8 V as compared to other filters such as BP filter, Hard filter, Serial filter, Soft filter, SG filter, and the TV filter.

Further evaluation of denoising filter performance from Fig. 13 showed that the WATV-Wiener filter improved SNR by about 4–30 dB compared to other denoising filters, consistent with our simulation study findings (5–20 dB). As noise might be present in the denoised signal from BP filter as observed from the healthy lung sound RMSE results in Fig. 12, which resulted in the large range of SNR improvement in adventitious lung sound signals from Fig. 13. WATV-Wiener improved SNR by about 44 dB in healthy lung sound signals, consistent with the SNR results in our simulation studies.

It is known that denoising continuous piecewise signal, e.g., healthy, and wheeze is more straightforward than denoising noncontinuous piecewise signal, e.g., crackle; however, we have achieved similar performance in terms of improved SNR, about 49 dB between crackle and wheeze in our experimental studies. From our experimental results, the WATV-Wiener filter functions better than the WATV filter in denoising noisy

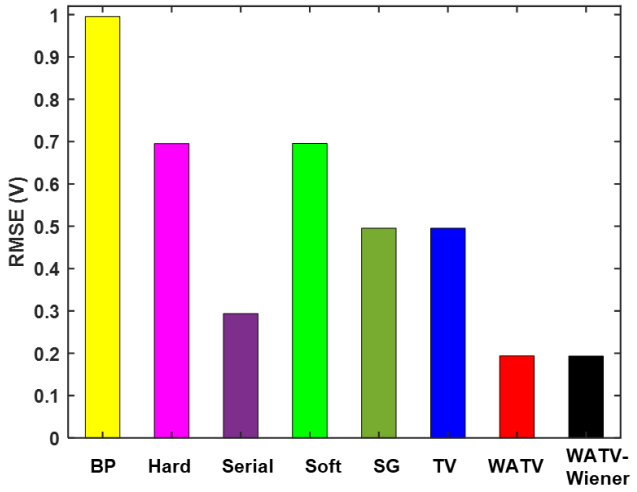

Fig. 12. Denoised filter RMSE performance in captured healthy lung sound signals.

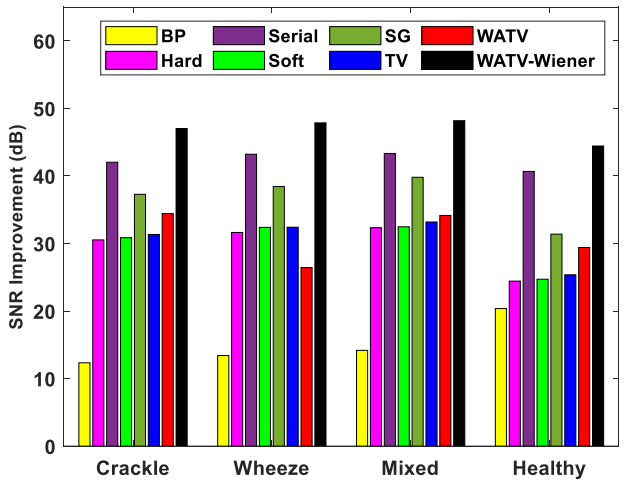

Fig. 13. Denoised filter SNR performance in actual healthy lung sound signals, and adventitious lung sound signals containing crackle, wheeze, or mixed of both crackle and wheeze.

signals achieving optimal RMSE, and improving the SNR, and the noise variance has minimal effect on WATV-Wiener.

We achieved better (optimal) RMSE results by 0.1–0.8 V in the actual healthy lung sound signals than other filters, similar to our simulation studies (0.2–0.9 V). Moreover, we achieved similar improved SNR for healthy lung sound signals between our simulation studies and experiment at about 3–20 dB with our optimal parameters. It can also be seen from the data in Fig. 13 that the improved SNR of about 4–30 dB was attained for adventitious (crackle, wheeze, mixed) lung sound signals. The improved SNR in our experiment studies (4–30 dB) is higher than the improved SNR in our simulation studies (5–20 dB) could be attributed to the modified computation of SNR as shown in (26), where noise is defined as the differences between denoised lung sound signals and observed noisy lung sound signals. Although a difference of 10 dB in improved SNR for crackle and wheeze is observed between our experiment and simulation studies, the minimal difference can be further reduced if noise data is available in the database. 'Noise data' is typically available in practice and usually referred to as using a sensor to capture the static electronic interference and ambient noise without lung sound signals, similar to our system's captured noise a_n in (25), and in the literature [3], [6], [18].

The optimal results obtained by the WATV-Wiener filter could be: 1) due to the advantage of wavelet-based denoising in noncontinuous piecewise signal, and 2) the optimal integration of two ideal filters, particularly in the RMSE sense, by addressing different challenges faced individually, e.g., WATV eliminates the requirement of selecting two different wavelet transform bases compared to empirical Wiener filter, but introduces artifacts, and empirical Wiener filter (known for eliminating artifacts through minimizing MSE) to remove the artifacts introduced by WATV [9], [14], [22].

In denoising actual lung sound signals, the WATV-Wiener filter algorithm comprises two primary filters: a bandpass filter ranging from 150 Hz to 1300 Hz and an integration of WATV and Wiener filter. Each step of the filter handles different components of noises. The FIR bandpass filter reduces most high-frequency and low-frequency noises such as cough, speech, and environment, which accounts for most of the noises in actual lung sound signals. However, with the overlapped noise frequency, a single linear filter cannot eliminate all the noise in the stopband [11], [18]. The WATV-Wiener filter segments the signal into different frequency regions in the wavelet domain and estimates all wavelet coefficients, both reliable and unreliable, in parallel, minimizing the denoised signal overall mean square error in the process of inverse filtering. The remaining high-frequency and low-frequency noises and environmental noise that has overlapping frequencies with signals of interest and are not removed by bandpass filter are reduced without distortion of the lung sounds, as shown in the results from Fig. 12 and Fig. 13.

In addition, the WATV-Wiener filter can identify the signal acoustic features of lung sounds in terms of RMSE, as shown in Fig. 12. Thus, the WATV-Wiener filter is helpful for further pattern recognition research and can help clinicians identify the condition of the patient's lungs based on observed acoustic features. Moreover, the WATV-Wiener filter enables the investigation and auscultation of several lung sounds that were previously inapplicable due to the weak acoustic features. The respiratory characteristics are often too weak to determine the condition of the lungs because of the inadequate ideal (noise-free) signal measuring environment. For instance, the WATV-Wiener filter helps expose the signals in relation to noise without compromising the characteristics of interest in the lung sound signals and makes denoised signals contain strong enough features in the judgment of lung conditions in terms of SNR, as shown in Fig. 13.

C. Limitations

However, some limitations must be considered with this work and potentially as future work. Firstly, on account of the overlapping frequency between lung sound signals and heart sound signals. This work focused on denoising environmental noises, while the separation of heart sound signals and lung sound signals was not considered. To obtain reference lung sound signals, the lung sound signals from both our measurement system and the shortlisted lung sound signals from the respiratory database were recorded on the patient's posterior to ensure that the heart sound signal will be minimal and does not interfere significantly with the lung sound signal. Additionally, 150 Hz – 1300 Hz bandpass filtering was applied to the actual lung sound signals to eliminate the lower heart sound frequency. While these frequency bands contain the majority of interesting lung sound characteristics, there can still be prominent unwanted heart sounds inside the frequency band. Therefore, to more accurately replicate the frequency overlap between heart sound signals and lung sound signals and assess the WATV-Wiener filter robustness in sound separation methods between lung and heart signals, pure and unfiltered reference lung and heart sound signals would be required.

The second correlated limitation is with the signal quality estimation of the respiratory database shown in (26). Although (26) strives to evaluate the denoised signal power in relation to noise quantitatively, it was not error-free. As noise is unavailable, the assumption for noise was made by subtracting the denoised signal from the original noisy signal. Hence, the differences between denoised lung sound signals SNR results from the respiratory database and the simulation studies can be explained with this limitation. The overall performance of the

WATV-Wiener filter does not directly consider if significant portions of the heart sound components are also being removed to obtain noise-free sounds. In the general utilization of the algorithm, the frequency domain of pulmonary sounds is relatively stable. The normalization wavelet method based on the signal power against noise significantly improves the integration of the WATV-Wiener filter. Besides, the integration of the WATV-Wiener filter proposed in this work shows a good effect in denoising without distortion.

VII. Conclusion

A controlled environment for capturing lung sound signals is not practical. The signals often contain interference such as ambient noise, leading to inaccurate lung health assessments. Hence, denoising is critical. Artifacts may be introduced when an unsuitable denoising filter is applied, particularly in the lung sound signals domain. Thus, we proposed a novel denoising wavelet-based approach by unifying the WATV filter and empirical Wiener filter denoising noisy lung sound signals in this paper. In contrast to parameter approximation akin to the literature, this paper established optimal filter parameters through case studies. Furthermore, the analysis from the case studies in this paper provided a new understanding of filter parameters affecting the overall filter denoising performance, particularly in the SNR domain. Subsequently, optimal RMSE performance is accomplished regardless of noise variance and verified in the simulation and experiment studies, ensuring the filter conserves waveform characteristics while denoising lung sound signals. Additionally, SNR improvement by about 3–20 dB and 4–30 dB was fulfilled and validated via simulation and experiment studies, respectively, compared with other accepted lung sound signals denoising filters in the literature. The research has demonstrated optimal denoising of noisy lung sound signals and further smoothing of the denoised signal achieving optimal RMSE results and improved SNR. This work is vital for a system that maps lung sound distribution or acoustic intensity signal into images for an accurate lung function assessment.

References

[1] L. E. Ellington et al., "Computerized lung sound analysis to improve the specificity of pediatric pneumonia diagnosis in resource-poor settings: protocol and methods for an observational study," *BMJ Open*, vol. 2, no. 1, p. e000506, 2012.

[2] A. Gurung, C. G. Scrafford, J. M. Tielsch, O. S. Levine, and W. Checkley, "Computerized lung sound analysis as diagnostic aid for the detection of abnormal lung sounds: A systematic review and meta-analysis," *Respiratory Medicine*, vol. 105, no. 9, pp. 1396-1403, 2011.

[3] E. Andrès, R. Gass, A. Charloux, C. Brandt, and A. Hentzler, "Respiratory sound analysis in the era of evidence-based medicine and the world of medicine 2.0," *Journal of Medicine and Life*, vol. 11, no. 2, pp. 89-106, Apr. 2018.

[4] P. Forgacs, "Crackles and wheezes," *The Lancet*, vol. 290, no. 7508, pp. 203-205, Jul. 1967.

[5] N. Meslier, G. Charbonneau, and J. L. Racineux, "Wheezes," *European Respiratory Journal*, vol. 8, no. 11, p. 1942, 1995.

[6] F. Meng, Y. Wang, Y. Shi, and H. Zhao, "A kind of integrated serial algorithms for noise reduction and characteristics expanding in respiratory sound," *International Journal of Biological Sciences*, vol. 15, no. 9, pp. 1921-1932, 2019.

[7] D. Emmanouilidou, E. D. McCollum, D. E. Park, and M. Elhilali, "Adaptive noise suppression of pediatric lung auscultations with real applications to noisy clinical settings in developing countries," *IEEE Transactions on Biomedical Engineering*, vol. 62, no. 9, pp. 2279-2288, 2015.

[8] R. Manwar, M. Zafar, and Q. Xu, "Signal and image processing in biomedical photoacoustic imaging: A review," *Optics,* vol. 2, no. 1, 2021.

[9] Y. Ding and I. W. Selesnick, "Artifact-free wavelet denoising: non-convex sparse regularization, convex optimization," *IEEE Signal Processing Letters*, vol. 22, no. 9, pp. 1364-1368, 2015.

[10] S. Ulukaya, G. Serbes, and Y. P. Kahya, "Performance comparison of wavelet based denoising methods on discontinuous adventitious lung sounds," in *39th Annual International Conference of the IEEE Engineering in Medicine and Biology Society (EMBC)*, 2017, pp. 2928-2931.

[11] D. Singh, B. K. Singh, and A. K. Behera, "Comparative study of different IIR filter for denoising lung sound," in *6th International Conference for Convergence in Technology (I2CT)*, 2021, pp. 1-3.

[12] N. S. Haider, R. Periyasamy, D. Joshi, and B. K. Singh, "Savitzky-Golay filter for denoising lung sound," *Brazilian Archives of Biology and Technology*, vol. 61, 2018.

[13] M. F. Syahputra, S. I. G. Situmeang, R. F. Rahmat, and R. Budiarto, "Noise reduction in breath sound files using wavelet transform based filter," *Materials Science and Engineering*, vol. 190, p. 012040, Apr. 2017.

[14] L. I. Rudin, S. Osher, and E. Fatemi, "Nonlinear total variation based noise removal algorithms," *Physica D: Nonlinear Phenomena*, vol. 60, no. 1, pp. 259-268, 1992/11/01/ 1992.

[15] M. Sarkar, R. Bhardwaz, I. Madabhavi, and M. Modi, "Physical signs in patients with chronic obstructive pulmonary disease," *Lung India : official organ of Indian Chest Society*, vol. 36, no. 1, pp. 38-47, Jan 2019.

[16] A. Bohadana, G. Izbicki, and S. S. Kraman, "Fundamentals of lung auscultation," *New England Journal of Medicine*, vol. 370, no. 8, pp. 744-751, Feb. 2014.

[17] T. Katila, P. Piirila, K. Kallio, E. Paajanen, T. Rosqvist, and A. R. Sovijarvi, "Original waveform of lung sound crackles: a case study of the effect of high-pass filtration," *Journal of Applied Physiology*, vol. 71, no. 6, pp. 2173-2177, Dec. 1991.

[18] D. Singh, B. K. Singh, and A. K. Behera, "Comparative analysis of lung sound denoising technique," in *First International Conference on Power, Control and Computing Technologies (ICPC2T)*, 2020, pp. 406-410.

[19] D. L. Donoho, I. M. Johnstone, G. Kerkyacharian, and D. Picard, "Wavelet shrinkage: Asymptopia?," *Journal of the Royal Statistical Society. Series B (Methodological)*, vol. 57, no. 2, pp. 301-369, 1995.

[20] D. L. Donoho, "De-noising by soft-thresholding," *IEEE Transactions on Information Theory*, vol. 41, no. 3, pp. 613-627, 1995.

[21] D. L. Donoho and I. M. Johnstone, "Ideal spatial adaptation by wavelet shrinkage," *Biometrika*, vol. 81, no. 3, pp. 425-455, 1994.

[22] P. G. Sandeep, M. S. Akbar, and G. B. Richard, "Improved wavelet denoising via empirical Wiener filtering," in *Proc.SPIE*, 1997, vol. 3169.

[23] N. Nikolaev, Z. Nikolov, A. Gotchev, and K. Egiazarian, "Wavelet domain Wiener filtering for ECG denoising using improved signal estimate," in *IEEE International Conference on Acoustics, Speech, and Signal Processing. Proceedings*, 2000, pp. 3578-3581.

[24] C. Hyeokho and R. Baraniuk, "Analysis of wavelet-domain Wiener filters," in *Proceedings of the IEEE-SP International Symposium on Time-Frequency and Time-Scale Analysis*, 1998, pp. 613-616.

[25] J. G. Gallaire and A. M. Sayeed, "Wavelet-based empirical Wiener filtering," in *Proceedings of the IEEE-SP International Symposium on Time-Frequency and Time-Scale Analysis*, 1998, pp. 641-644.

[26] M. Hsueh, H. Wu, and B. Lu, "The evaluation system for the computer simulation of the crackles in respirations," in *21st International Conference on Advanced Communication Technology (ICACT)*, 2019, pp. 583-588.
[27] B. Lu, M. Liu, M. Hsueh, P. Lin, X. W. Li, and H. Wu, "Preliminary study on production of coarse and fine crackles in respiration using a model of communication theory," in *22nd International Conference on Advanced Communication Technology (ICACT)*, 2020, pp. 461-464.
[28] B.-Y. Lu, H.-D. Wu, S.-R. Shih, F.-C. Chong, M.-L. Hsueh, and Y.-L. Chen, "Combination of frequency and amplitude-modulated model for the synthesis of normal and wheezing sounds," *Australasian Physical & Engineering Sciences in Medicine*, vol. 34, no. 4, pp. 449-457, Dec. 2011.
[29] R. L. H. Murphy, S. K. Holford, and W. C. Knowler, "Visual lung sound characterization by time-expanded wave-form analysis," *New England Journal of Medicine*, vol. 296, no. 17, pp. 968-971, Apr. 1977.
[30] D. F. Ponte, R. Moraes, D. C. Hizume, and A. M. Alencar, "Characterization of crackles from patients with fibrosis, heart failure and pneumonia," *Medical Engineering & Physics*, vol. 35, no. 4, pp. 448-456, Apr. 2013.
[31] H. Kiyokawa, M. Greenberg, K. Shirota, and H. Pasterkamp, "Auditory Detection of Simulated Crackles in Breath Sounds," *Chest*, vol. 119, no. 6, pp. 1886-1892, Jun. 2001.
[32] Y. Wu, G. Gao, and C. Cui, "Improved wavelet denoising by non-convex sparse regularization under double wavelet domains," *IEEE Access*, vol. 7, pp. 30659-30671, 2019.
[33] J. L. Darbyshire, M. Müller-Trapet, J. Cheer, F. M. Fazi, and J. D. Young, "Mapping sources of noise in an intensive care unit," *Anaesthesia*, vol. 74, no. 8, pp. 1018-1025, Aug. 2019.
[34] B. M. Rocha et al., "An open access database for the evaluation of respiratory sound classification algorithms," *Physiological Measurement*, vol. 40, no. 3, p. 035001, Mar. 2019.
[35] Garcia, Damien. "Robust smoothing of gridded data in one and higher dimensions with missing values." *Computational Statistics and Data Analysis*, vol. 54, no. 4, Apr. 2010, pp. 1167–78.
[36] S. R. Messer, J. Agzarian, and D. Abbott, "Optimal wavelet denoising for phonocardiograms," *Microelectronics Journal*, vol. 32, no. 12, pp. 931-941, Dec. 2001.

Chang Sheng Lee received the B.Eng. degree in mechatronics engineering from University of Glasgow, United Kingdom, in 2013 and the M.Sc. degree in mechanical engineering from National University of Singapore, Singapore, in 2016. He is currently pursuing the Ph.D. degree in electrical engineering at University of Glasgow, United Kingdom. He is currently in the Global Technology Integration department with Hill-Rom Services Pte Ltd, Singapore as a Research Engineer. His Ph.D. work is focused on the development of sensing technologies and system for lung health assessment.

Minghui Li (M'08-SM'22) received the B.Eng. and M.Eng. degrees from Xidian University, Xi'an, China, in 1994 and 1999, respectively, and the Ph.D. degree from Nanyang Technological University (NTU), Singapore, in 2004, all in electrical engineering. From 1994 to 1996, he was a Faculty Member with the School of Electronic Engineering, Xidian University. From 1999 to 2000, he was a Research Engineer with SIEMENS (China) Co., Ltd., Beijing, China. From 2003 to 2008, he was first with the School of Electrical and Electronic Engineering and then with the Intelligent Systems Center, Nanyang Technological University (NTU) as a Research Fellow. From 2008 to 2013, he was a Lecturer with the Department of Electronic and Electrical Engineering, University of Strathclyde, U.K. He joined the James Watt School of Engineering, University of Glasgow, U.K., as an Associate Professor in August 2013. His research interests include phased array systems, array design and processing, direction-of-arrival estimation, adaptive and arbitrary beamforming, spatial-temporal processing and coding, smart antennas, MIMO, evolutionary computation, wireless sensor networks, and coded ultrasound, with application to modern radar, underwater sonar, medical diagnosis, non-destructive evaluation, and wireless communications.

Yaolong Lou (S'94–M'97–SM'11) received the B.Eng. and M.Eng. degrees from Harbin Institute of Technology, Harbin, China, in 1985 and 1988, respectively, and the *Dr.-Ing.* degree from The University of Wuppertal, Wuppertal, Germany, in 1996, all in electrical engineering. From 1997 to 1998, he was a Postdoctoral Fellow with the National University of Singapore. From 1999 to 2003, he was first a Senior Engineer then a Principal Engineer with Singapore Research Laboratory of Sony Electronics. From 2003 to 2005, he was a Chief Engineer with Philips Electronics in Singapore. From 2006 to 2007, he was a Staff Engineer with Seagate Technology International in Singapore. Since 2007, he has been with Welch Allyn later Hill-Rom in Singapore as Principal Engineer, R&D Manager and Senior Manager for Innovation in Global Technology Integration department. Dr. Lou's areas of expertise include small and special electrical machines and their controls, motion control systems, intelligent control with neural networks; system analysis, modeling, and simulation; as well as medical devices and image processing for cardiovascular and respiratory systems and vision care systems.

Ravinder Dahiya (Fellow, IEEE) is currently Professor of electronics and nanoengineering at the University of Glasgow, U.K. He is the Leader of the Bendable Electronics and Sensing Technologies (BEST) Research Group. His group conducts fundamental and applied research in the multidisciplinary fields of flexible and printable electronics, tactile sensing, electronic skin, robotics, and wearable systems. He has authored over 400 research articles, 8 books and 15 submitted/granted patents and disclosures. He has led several international projects. He is the President of IEEE Sensors Council and Founding Editor-in-Chief of IEEE JOURNAL ON FLEXIBLE ELECTRONICS (J-FLEX). He has served on the Editorial Boards of Scientific Reports, IEEE SENSORS JOURNAL, and the IEEE TRANSACTIONS ON ROBOTICS. He was Distinguished Lecturer of IEEE Sensors Council during 2016-2021. He has been the General Chair and Technical Program Chair of several conferences. He has received the prestigious EPSRC fellowship, the Marie Curie Fellowship, and the Japanese Monbusho Fellowship. He has received several awards, including 12 best journal/conference paper awards as author/co-author, 2016 Microelectronic Engineering Young Investigator Award and the 2016 Technical Achievement Award from the IEEE Sensors Council.